Available online at www.sciencedirect.com
SCIENCE DIRECT®
Engineering Geology 73 (2004) 71–91
ENGINEERING GEOLOGY
www.elsevier.com/locate/enggeo

Influence of petrographic parameters on geotechnical properties of tertiary sandstones from Taiwan

F.S. Jeng*, M.C. Weng, M.L. Lin, T.H. Huang

Department of Civil Engineering, National Taiwan University, Taipei, Taiwan

Received 13 November 2002; accepted 3 December 2003

Abstract

While tunneling through Tertiary sandstones in Taiwan, tunnel squeezing occurred in some of the sandstones (e.g., Mucha Tunnel and Chungho Tunnel in northern Taiwan), but not in all of them. This phenomenon indicates that the geotechnical properties of Tertiary sandstones differ from one sandstone to another, and further characterization is of interest. Laboratory experiments were conducted to explore the geotechnical characteristics, including strength, deformational behavior and wetting softening phenomena, of more than 13 Tertiary sandstones from northern Taiwan. It was found that these sandstones differ from hard rocks in having significant shear dilation and wetting softening behavior, which is defined as the reduction of both strength and stiffness of dry sandstone due to wetting. Such distinct behavior can occur even when the sandstones have medium to moderate strength. Based on the degree of wetting softening behavior as well as the deformational behavior, two types of sandstones, *types A* and *B*, were identified. Relative to *type A* sandstone, the *type B* sandstone is characterized by more deformation, shear dilation and more significant wetting softening.

In addition, how the microscopic parameters (or petrographic parameters) affect the macroscopic mechanical behavior, including the deformational behavior, uniaxial compressive strength (UCS) and strength reduction (R) due to wetting, was studied by petrographic analysis. Among the petrographic and physical parameters evaluated, the grain area ratio (GAR) and porosity are found to be the key parameters. As a result, empirical relations of UCS and strength reduction (R) due to wetting, expressed in terms of porosity and grain area ratio, respectively, are proposed. Comparisons were made to sandstones worldwide from published data, and it is found that these two empirical relations are also applicable to other sandstones.

Finally, a classification method, based on UCS and R on the one hand and the petrographic parameters (grain area ratio and porosity) on the other, is proposed for Tertiary sandstones to indicate the geotechnical characteristics of sandstones. This proposed classification method can also be expressed in terms of grain–matrix–porosity content of sandstones. It is also found that porosity has more influence on the UCS than grain and matrix content does.

Keywords: Tertiary sandstone; Characterization; Petrographic parameter; GAR; Wetting softening

1. Introduction

Most of the rocks in western Taiwan are Tertiary weak rocks, including sandstone, shale and mudstone. They are not strong enough and cannot be classified as hard rock as a result of a relatively short rock

* Corresponding author. Tel.: +886-2-2363-0530; fax: +886-2-2364-5734.
E-mail address: fsjeng@ntu.edu.tw (F.S. Jeng).

0013-7952/$ - see front matter © 2004 Elsevier B.V. All rights reserved.
doi:10.1016/j.enggeo.2003.12.001

forming period. The typical strength ranges from 10 to 80 MPa (Jeng et al., 1994).

While tunneling through the Tertiary rock strata in northern Taiwan, difficulties including severe squeezing and raveling were encountered in some of the strata (Jeng et al., 1996b). Crown settlements ranging from 14 to 30 cm occurred in several strata of the Tertiary sandstones. However, not all the Tertiary strata are problematic. The crown settlements are normally several centimeters in most Tertiary strata. Therefore, it is of interest to identify what Tertiary rocks are problematic. And why?

It has been found that the problematic strata do not necessarily have the lowest strength; therefore, other properties of the Tertiary rock causing tunnel squeezing are of interest. For instance, some of the squeezing occurred after the top heading of the entire tunnel was fully excavated. This phenomenon implies that the time-dependent deformation and/or the reduction of strength of Tertiary rock may also account for the squeezing. Jeng et al. (1996b) reviewed those unsuccessful cases and found that the causes of squeezing were potentially related to the following characteristics of Tertiary rocks, and further study is necessary:

(a) Wetting softening of sandstone—The humidity within the tunnel as well as seeping water may significantly reduce the strength and the stiffness of sandstone. Investigation about the influence of wetting indicated that, when a dry sandstone is

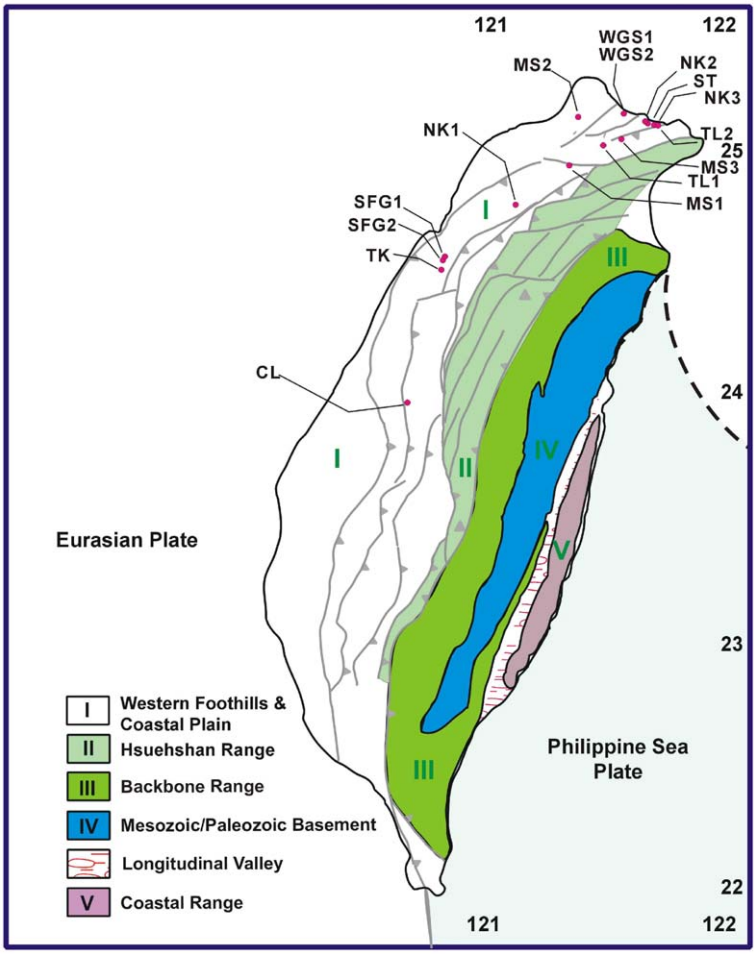

Fig. 1. Geological map of Taiwan and locations of samples.

Table 1
Lithological characteristics of the sandstones studied

Formation	Classification (Pettijohn et al., 1987)	Geological age	Sedimentary facies	Remark
WGS1	Lithic graywacke	Oligocene	Marine-terrestrial mixed facies	
WGS2	Lithic graywacke	Oligocene	Marine-terrestrial mixed facies	Apparent preferred orientation
MS1	Lithic graywacke	Miocene	Littoral facies	
MS2	Lithic graywacke	Miocene	Littoral facies	
MS3	Lithic graywacke	Miocene	Littoral facies	Apparent preferred orientation
TL1	Lithic graywacke	Miocene	Marine facies	
TL2	Lithic graywacke	Miocene	Marine facies	
ST	Lithic graywacke	Miocene	Littoral facies	
NK	Lithic graywacke	Miocene	Marine facies	
TK	Lithic graywacke	Miocene	Littoral facies	Apparent preferred orientation
SFG1	Quartzwacke	Miocene	Littoral facies	
SFG2	Lithic graywacke	Miocene	Littoral facies	Apparent preferred orientation, rich in mica content
CL	Lithic graywacke	Pliocene	Littoral facies	Rich calcite content
Fell	Quartz arenite	–	–	Bell (1978)
LSF/NCSF	–	Triassic	–	Bell and Culshaw (1993)
Sneinton	–	–	–	Bell and Culshaw (1998)
Mariannhill	Arkose	Silurian	Terrestrial facies	Bell and Culshaw (1998)
–	Litharenite sandstone	Upper Carboniferous	–	Ulusay et al. (1994)

soaked in water for 120 min, the decreases in the compressive strength, shear modulus and bulk modulus values are 60%, 60% and 70%, respectively (Jeng et al., 1996a). The wetting softening of sandstone directly contributes to the excessive crown settlement during tunnel excavation.

(b) Shear dilation—Before the rock approaches its failure state during excavation, it is often considered to be elastic and the inelastic deformation is negligible prior to the pre-peak stage of loading. This point of view can be adequate in case of hard rocks; however, for Tertiary rocks, this assertion is not necessarily valid. Theoretically, shearing of an isotropic elastic rock will not induce volumetric dilation, which inherently contributes to the tunnel squeezing. However, shear dilation of weak rock has been reported in several publications (Handin and Hager, 1957;

Table 2
Physical and petrographical properties of the sandstones studied

Formation	γ_d (g/cm^3)	G_s	n (%)	GAR (%)	Matrix (%)	PD (%)	Mineralogy of grains			FF
							Quartz (%)	Feldspar (%)	Rock fragment (%)	
WGS1	2.19	2.66	17.4	65.0	17.6	68.9	90.3	0.0	9.7	0.61
WGS2	2.26	2.72	16.7	25.3	58.0	44.9	85.8	0.0	7.2	0.62
MS1	2.24	2.52	11.5	50.4	38.2	–	88.0	0.2	10.3	0.62
MS2	2.28	2.66	14.1	67.5	18.5	74.2	90.7	0.2	9.0	0.60
MS3	2.32	2.67	13.1	51.0	35.9	65.4	85.0	2.3	12.2	0.62
TL1	2.36	2.72	13.1	36.4	50.5	56.2	86.5	1.7	9.9	0.64
TL2	2.35	2.70	12.8	50.0	37.2	67.0	87.3	0.7	9.7	0.62
ST	2.18	2.67	18.2	40.4	41.4	57.4	77.7	4.4	12.7	0.63
NK	2.31	2.71	14.8	28.6	56.6	55.2	90.0	2.3	5.6	0.63
TK	2.30	2.65	12.8	28.2	59.0	49.4	84.5	0.5	13.0	0.63
SFG1	2.01	2.66	24.6	52.6	22.8	73.6	95.6	0.8	3.0	0.62
SFG2	2.21	2.66	16.9	42.8	40.4	65.4	78.4	1.6	8.9	0.58
CL	2.14	2.70	20.7	39.4	40.0	61.2	83.7	1.0	5.5	0.63

Remarks: γ_d = dry density of sandstone, G_s = specific weight, n = total porosity, GAR = grain area ratio, PD = packing density, FF = form factor.

Dyke and Dobereiner, 1991; Aristorenas, 1992; Bernabe et al., 1994; Jeng and Huang, 1998a; Besulle et al., 2000; Jeng et al., 2002).

(c) Creep of rock—Based on an experimental study (Jeng and Huang, 1998b), the rock, in the locations where squeezing occurs, also exhibits significant creep behavior.

The purpose here is to investigate the short-term (time-independent) deformational behavior, including shear dilation as well as the wetting softening, which inherently causes problems in geotechnical engineering, e.g., excess crown settlement while tunneling.

On the other hand, what accounts for the discrepancies of the mechanical behavior of sandstones is of great interests to researchers. Therefore, the petrographic features of sandstones have been of concern (Kahn, 1956; Bell, 1978; Dobereiner and De Freitas, 1986; Pettijohn et al., 1987; Shakoor and Bonelli, 1991; Bell and Culshaw, 1993; Hawkins and McConnell, 1992; Ulusay et al., 1994; Hatzor and Plachik, 1997, 1998; Lin and Hsiuang, 1998; Bell and Lindsay, 1999; Tuğrul and Zarif, 1998, 1999). The petrographic parameters studied include: (a) the mineral composition of grains and matrix; (b) the degree of packing of sandstone, which can be expressed in terms of packing

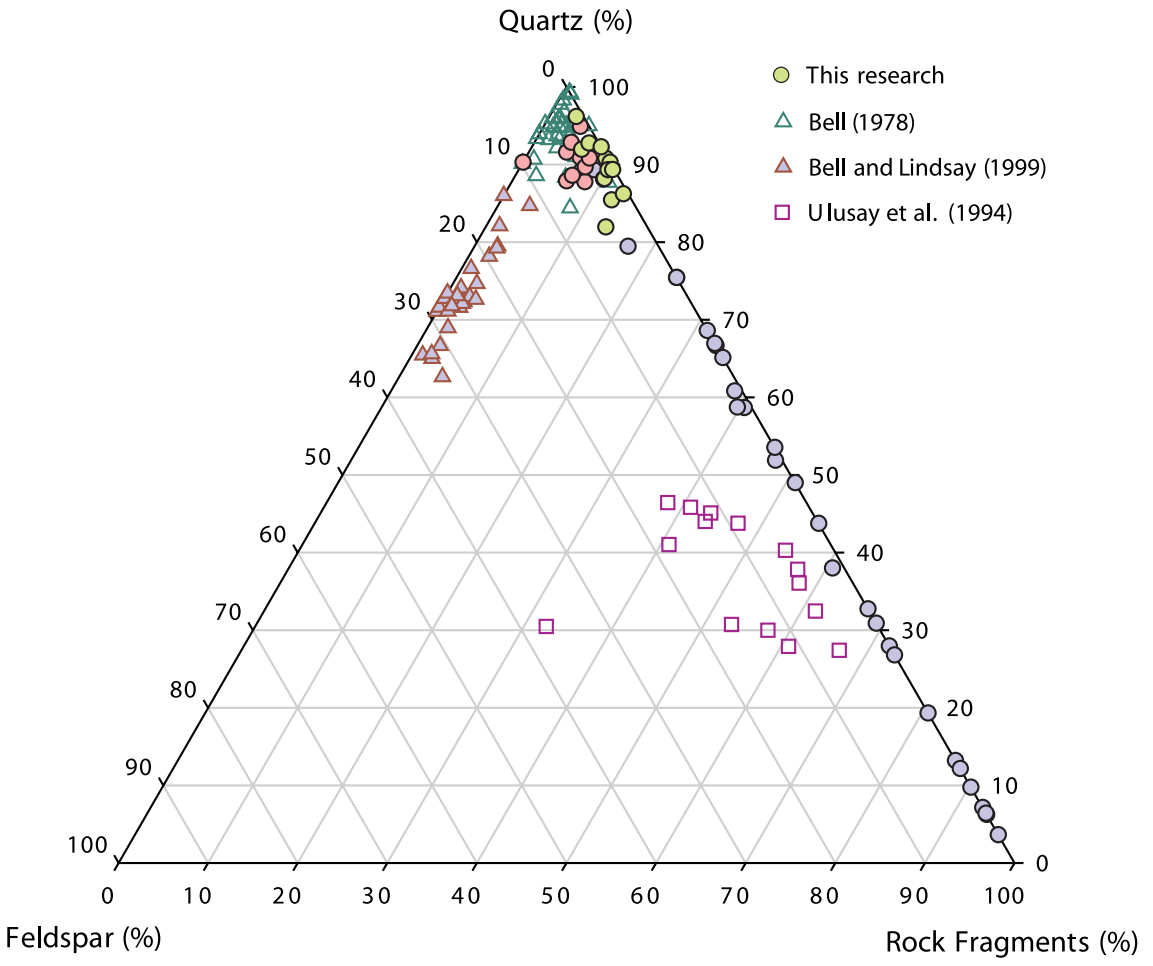

Fig. 2. Grain composition of the studied sandstones based on Pettijohn's classification (1987). Information of sandstones published by other researchers is also included for comparative purposes. The studied sandstones are characterized with high quartz content and almost no feldspar content.

density (PD), grain contact (GC), grain area ratio (GAR) or porosity (n) and (c) the type of grain contact.

The mineral composition may influence the strength of sandstones. It has been found that the increase of quartz content either has no influence on the strength of sandstone (Bell, 1978; Dobereiner and De Freitas, 1986), or it increases somewhat the strength of some sandstones from South Africa (Bell and Lindsay, 1999).

According to Dobereiner and De Freitas (1986), greater grain contact (instead of packing density) results in greater strength of saturated sandstone, and saturated strength of 20 MPa may serve for the upper bound strength of weak rock, beyond which the failure of rock is mainly controlled by the grain fracturing instead of the rolling of grains. Moreover, it also has been found that greater packing density does enable greater strength (Bell, 1978; Bell and Culshaw, 1993). It has been reported that the textural characteristics appear to be more important than mineral composition to the mechanical behavior of sandstone (Ulusay et al., 1994).

For rocks other than sandstone, studies on dolomite (Hatzor and Plachik, 1997, 1998) showed that a denser (less porosity) or a finer (a smaller grain size) texture of dolomite resulted in greater strength. As for sandstones, it has been reported that only porosity, and not the grain size, has meaningful influence on the strength of sandstone (Plachik, 1999).

The presence of moisture may also influence the uniaxial compressive strength (UCS) of sandstone. It has been shown that moisture decreases the UCS of

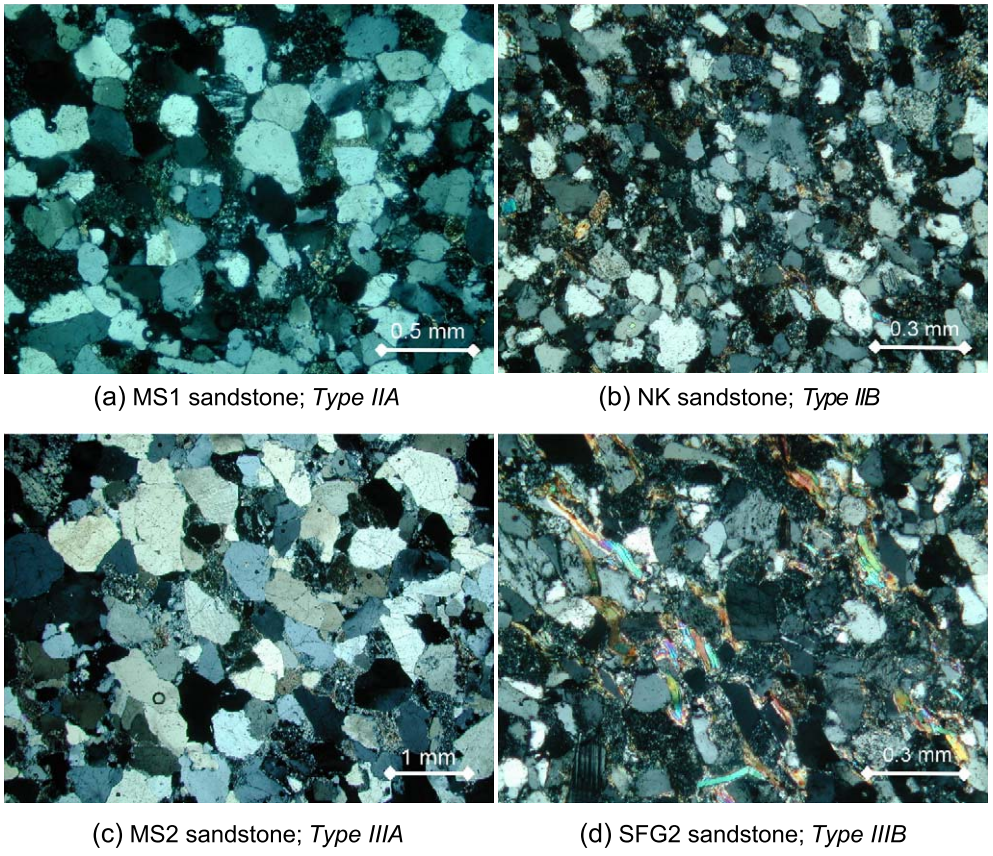

(a) MS1 sandstone; *Type IIA* (b) NK sandstone; *Type IIB*

(c) MS2 sandstone; *Type IIIA* (d) SFG2 sandstone; *Type IIIB*

Fig. 3. Some of the typical petrographic images (crossed nickel) of the studied sandstones. The scale of each image is shown by a white bar. The symbols MS1, MS2, NK and SFG2 represent the stratum formation where the specimens came from, as listed in Table 1 and with locations shown in Fig. 1. The rock types are defined by Fig. 9b.

weaker sandstones (Dyke and Dobereiner, 1991) and even strong sandstones (Hawkins and McConnell, 1992).

Since it has been shown that the petrographic parameters do affect the physical and mechanical behavior of sandstone, the influence of petrographic parameters was also evaluated in this research. As the studied Tertiary sandstones exhibit significant wetting softening behavior, in addition to the strength of sandstone examined by the previous researches, the influence of the petrographic parameters on the wetting softening behavior was also evaluated.

On the other hand, since the mechanical properties of sandstones can be affected by several of the above-mentioned parameters, the influence of each parameter should be clarified beforehand in order to highlight which are the key parameters. In addition to the multivariate regression method (e.g., Ulusay et al., 1994), a stepwise iteration method, which is capable of extracting the influence of key parameters one by one, is proposed.

2. Experimental setup

A total of 13 sandstones, obtained from 8 different geological formations, were sampled from northern and western Taiwan within the Western Foothill Range, as shown in Fig. 1. As listed in Table 1, these sandstones were deposited under marine, marine–terrestrial and littoral sedimentary environments, and their geological ages ranged from Oligocene to Pliocene (Ho, 1986). The specimens were cored in laboratory from rock blocks excavated from each of the formations. Such a method of core recovery has also been adopted by other researchers (Shakoor and Bonelli, 1991; Hawkins and McConnell, 1992). In this way, the spatial variation in the mechanical properties of specimens can be minimized and specimens possibly with different qualities (e.g., weathered sandstone) can be screened out in advance by visual examination as well. Furthermore, each test to measure a given property was performed at least three times on each formation and the mean value of measured data was then set to represent the property of each formation.

The physical properties, including dry density (γ_d), specific gravity (G_s), water content (w) and porosity (n), of sandstones were measured in accordance with the testing procedures suggested by ISRM (1981). The porosity measured was selected to be "total porosity," which is determined by the following formula,

$$n = 1 - (\gamma_d / G_s) \quad (1)$$

Since other researchers (Bell, 1978; Ulusay et al., 1994; Bell and Lindsay, 1999) also adopted same

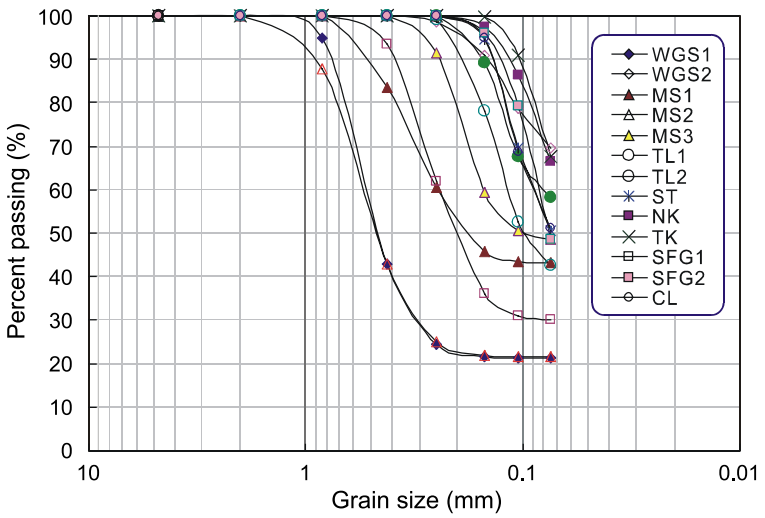

Fig. 4. Grain size distribution of the studied sandstones.

Table 3
Mineral content of the matrix for each type of sandstone

Formation	Illite (%)	Kaolinite (%)	Chlorite (%)	Montmorillite (%)	Mixed layer (%)	Type[a]
WGS1	72	14	2	4	8	IIIA
WGS2	73	3	0	15	9	IIB
MS1	39	50	11	0	–	IIA
MS2	75	7	1	4	13	IIIA
MS3	69	11	19	0	–	IIA
TL1	32	14	6	6	42	IIB
TL2	16	30	54	0	–	IIA
ST	21	64	15	0	–	IIIB
NK	46	44	10	0	–	IIB
TK	60	40	1	0	–	IIB
SFG1	17	59	23	1	–	IVA
SFG2	20	56	24	0	–	IIIB
CL	35	8	3	27	27	IIIB

[a] Fig. 9 defines the types of sandstone and the strength types (I, II, III and IV) are classified based on ISRM (1981).

measure of porosity, the results of this research and theirs could be compared on a consistent basis.

The specimen size was 5.5 cm in diameter and 12.5 cm in height for all tests and all specimens were oven-dried (105 °C). Both uniaxial compression tests and triaxial tests (TC), following ISRM suggested procedures, were conducted to obtain the strength of sandstones. Meanwhile, to separate the deformation induced during loading of hydrostatic stress $(p = \sigma_{11} + \sigma_{22} + \sigma_{33}/3) = (I_1/3)$ and shear stress $\sqrt{J_2} = \sqrt{1/2\, S_{ij}S_{ij}}$, $S_{ij} =$ second deviatoric stress tensor), stress-path control tests, the so-called pure shear tests (referred as PS) (Jeng et al., 2002), were also carried out. In those tests, the stress-path was controlled and composed of two stages: (a) increases of hydrostatic stress with zero shear stress; followed by (b) increases of shear stress with hydrostatic stress unchanged so that the volumetric strain induced by hydrostatic stress and by shear stress could be separated and the shear strain induced by shear stress could be measured as well.

The triaxial cell was able to sustain the confining pressure up to 175 MPa. A pressure transducer monitored the confining pressure with an accuracy of 0.1 MPa. The axial load was provided by a servo-controlled high stiffness MTS machine, which has a maximum load and stiffness of 4448 kN and 13.1×10^9 N/m, respectively. The load was applied at a rate of 5 MPa/min.

The longitudinal and transverse types of deformation were separately measured by a full Wheatstone bridge consisting of four strain gages, which were capable of measuring strains up to 2% with an accuracy of ± 0.85 (μm/m)/°C.

Since some of the Tertiary sandstones exhibit wetting softening behavior, experiments were conducted both on dry and wet specimens. To enable a constant wetting condition, the sandstones were soaked in water in a vacuum chamber for sufficient length of time (at

Table 4
Mechanical propmerties of sandstones

Formation	UCS_{dry} (MPa)	UCS_{wet} (MPa)	R	Strength classification ISRM (1981)	E_{dry} (MPa)	E_{wet} (MPa)	E_{wet}/E_{dry}	No. of specimens	
								Dry	Sat
WGS1	34.1	25.4	0.74	Moderate	11.9	4.4	0.37	8	9
WGS2	47.5	6.7	0.14	Moderate	5.0	1.6	0.32	10	8
MS1	48.5	28.9	0.60	Moderate	7.6	3.4	0.45	15	2
MS2	37.1	28.3	0.76	Moderate	12.7	10.0	0.79	27	23
MS3	82.7	43.3	0.52	Medium	14.0	9.9	0.71	3	3
TL1	68.7	23.2	0.34	Medium	9.7	4.3	0.44	11	9
TL2	77.5	44.2	0.57	Medium	12.2	7.3	0.60	3	3
ST	38.4	7.8	0.20	Moderate	5.6	1.6	0.29	5	3
NK	86.0	43.2	0.50	Medium	12.1	8.1	0.67	4	3
TK	69.0	29.4	0.43	Medium	5.2	2.2	0.43	10	2
SFG1	14.5	12.2	0.84	Low strength	2.6	2.2	0.85	3	3
SFG2	46.4	19.9	0.43	Moderate	5.2	2.5	0.48	3	3
CL	19.9	3.1	0.16	Low strength	–	–	–	7	6

Remarks: The strength reduction ratio R due to wetting softening is defined as: $R = UCS_{wet}/UCS_{dry}$.

least 24 h) so that the water content would stop increasing. In this way, water was allowed to fill all the coalescent pores. The point should be made that the specimens should not be submerged in water for too long to avoid dissolving and leaching of the minerals especially for the sandstones containing calcite as matrix material. During the triaxial tests, back water pressure of 0.5–1 MPa was applied to increase the degree of saturation. Since the unaxial compressive strength of wet sandstone (UCS_{wet}) is often lower than that of dry sandstone (UCS_{dry}), a measure R (strength reduction ratio indicating the reduction of strength due to wetting) is defined as:

$$R = UCS_{wet}/UCS_{dry} \quad (2)$$

To observe the petrographic features of the studied sandstones, at least one thin section was prepared for each formation. The texture of sandstone was then observed under microscope under the conditions of direct reflection, open nicols, crossed nicols and crossed nicols with a λ-plate, followed by taking photos from five areas within the section. The λ-plate

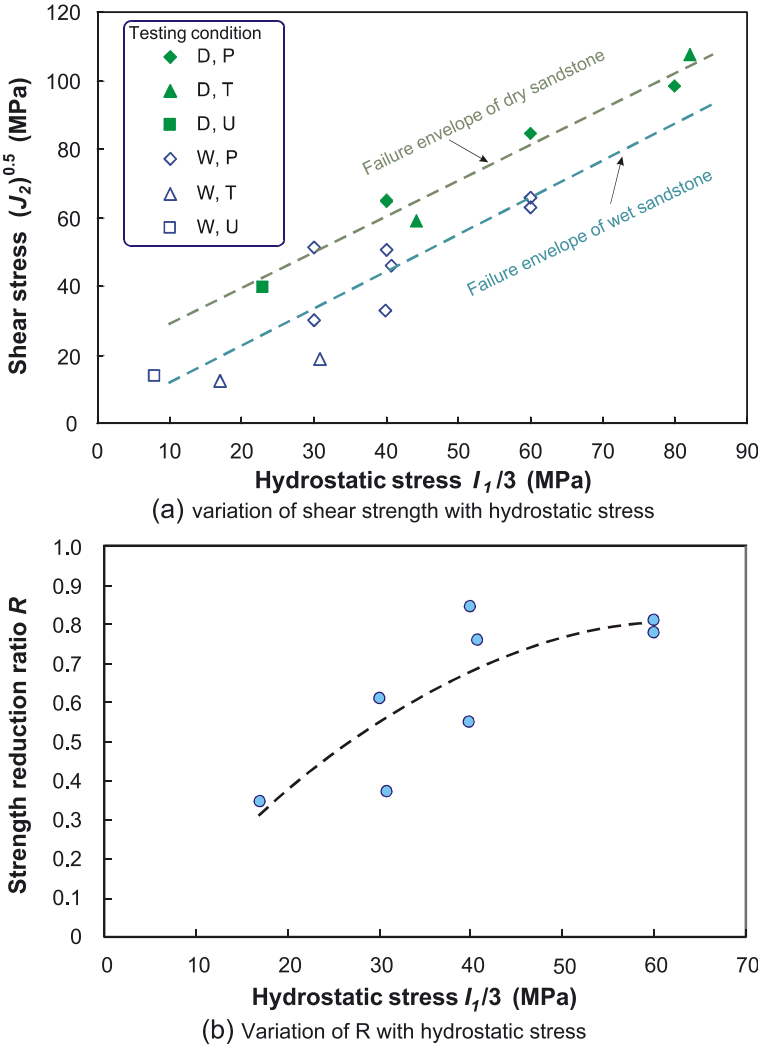

Fig. 5. Typical strength of the studied sandstone. All the specimens were sampled from TL1 formation, which properties shown in Tables 1 and 2. D = dry specimen, W = wet specimen, P = pure shear test, T = triaxial compressive test, U = uniaxial compression test.

was adopted in order to enable a much better color contrast between grains, which is helpful for subsequent processes of identifying the grain boundary. Utilization of computer software (Image Pro Plus) enables overlaying of the corresponding images and facilitates the determination of individual grain boundaries. As a result, the boundaries of grains and the mineral composition of grains can be identified both by computer software and by visual observation. Moreover, the size of area of observation is set to include 80–150 grains in an image, so that representative petrographic features can be observed from each area.

The features of grains, including their areas, perimeters, diameters and axis lengths, were measured. Meanwhile, the GAR, defined by Ersoy and Waller (1995), which represents the percentage of grain within rock and is found to be a key parameter in later analyses, was also adopted.

Since grains, matrix and porosity constitute the whole sandstone, the following relationship can be obtained:

$$\text{GAR} + \text{matrix content} + \text{porosity } (n) = 100\% \quad (3)$$

Therefore, the matrix content was not directly measured, but calculated from Eq. (3) and by the measured GAR and total porosity.

Other petrographic features including GC, PD and type of grain contact, which have been shown to have influence on the mechanical behavior of sandstone (Bell, 1978; Dobereiner and De Freitas, 1986; Shakoor and Bonelli, 1991; Bell and Culshaw, 1993, 1998; Ulusay et al., 1994; Bell and Lindsay, 1999), were also measured in this research. The detailed definition and determination of the petrographic parameters used in the work are presented in Appendix A.

Meanwhile, for the studied sandstones, it was found that both GC and PD were strongly related to gain area ratio, which can be expressed in terms of grain area ratio by the following equations:

$$\text{GC} = 1.54\ \text{GAR} - 67.7\% \quad (r^2 = 0.900) \quad (4)$$

$$\text{PD} = 0.58\ \text{GAR} - 36.2\% \quad (r^2 = 0.804) \quad (5)$$

Based on Eqs. (4) and (5), sandstones with more grain area ratio tend to have a greater grain contact and a greater packing density. Accordingly, in the subsequent analyses, among these three parameters,

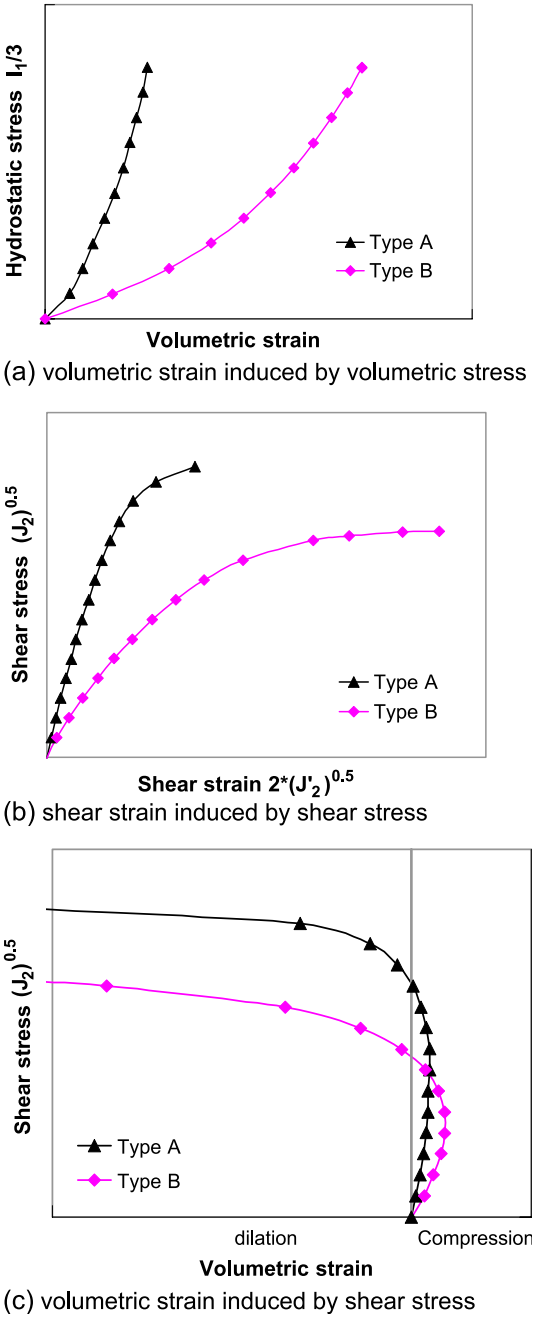

Fig. 6. Typical deformational behavior of the studied Tertiary sandstones. In this figure, *types A* and *B* sandstones are sampled from MS2 and WGS2 formations, respectively. J_2' ($=1/2 e_{ij}e_{ij}$, e_{ij} = second deviatoric strain tensor) is a measure of shear strain.

Table 5
Correlations of the parameters likely to affect geotechnical properties of sandstones

r / r^2		Dry density	Gs	Porosity	Quartz	Feldspar	Rock fragment	*GAR*	d_{mean}	FF
		(g/cm^3)		(%)	(%)	(%)	(%)	(%)	(mm)	
Dry density	(g/cm^3)		0.178	0.875	0.025	0.314	0.015	0.054	0.127	0.022
				0.110	0.317	0.216	0.114	0.310	0.241	0.043
Gs		0.422			0.154	0.463	0.011	0.047	0.288	0.003
Porosity	(%)	–0.936	–0.331			0.376	0.552	0.367	0.575	0.320
Quartz	(%)	0.159	–0.563	–0.393			0.248	0.191	0.310	0.016
Feldspar	(%)	0.561	–0.464	–0.680	0.613			0.004	0.068	0.069
Rock fragment	(%)	–0.123	–0.337	0.104	–0.743	–0.498			0.622	0.241
GAR	(%)	0.232	–0.557	–0.217	0.709	0.437	0.064			
d_{mean}	(mm)	0.357	0.491	–0.537	0.758	0.557	0.260	0.788		0.293
FF		0.148	0.206	0.057	–0.566	–0.127	–0.263	–0.491	–0.541	

only grain area ratio was adopted since it directly represents the two-dimensional texture of sandstones and it can be obtained with less visual judgment as compared with the process of obtaining grain contact or packing density.

To study the relative mineral composition of matrix, both non-quantitative and semi-quantitative X-ray diffraction tests (XRD) were also conducted. Consequently, the relative mineral composition of matrix could be identified.

3. Physical and mechanical properties of the studied sandstones

The physical properties of the sandstones studied are summarized in Table 2. In general, the studied sandstones are mainly composed of quartz and rock fragments and have very little of feldspar (less than 5%), as shown in Fig. 2; accordingly, these sandstones can be classified as lithic greywacke or quartzwacke based on Pettijohn's definition (Pettijohn et al., 1987). The sandstones reported by Ulusay et al. (1994) are similar to the Tertiary sandstones of this research but have a greater content of feldspar (about 5–15%). The sandstones reported by Bell (1978) and Bell and Lindsay (1999) have very little content of rock fragments (less than 10%). The geotechnical characteristics of all these sandstones, with different mineral compositions, will be further compared.

Fig. 3 illustrates some of the petrographic images of the sandstones. In general, the grains have sub-rounded to sub-angular geometry. Some of the sandstones have a rather small grain ratio (GAR < 50%), which indicates that more than a half of the area is filled with matrix material and porosity.

The studied sandstones have a fairly wide spectrum of grain sizes. The grain size distributions are shown in Fig. 4, indicating that the studied sandstones have up to one order of difference in grain sizes. The grain size distribution was obtained by recording the sizes of all grains in a reference area of a thin section, sorting the sizes and calculating the accumulative distribution. It was noticed that the finer the sandstone, the greater the matrix content.

The relative mineral composition of the matrix for all sandstones is summarized in Table 3. The matrix is mainly composed of the illite, kaolinite and

Table 6
Correlations of UCS with the other parameters

r^2	G_s	Porosity (%)	Quartz (%)	Feldspar (%)	Rock fragment (%)	GAR (%)	d_{mean} (mm)	FF
UCS_{dry} (MPa)	0.131	0.702	0.537	0.430	0.596	0.001	0.019	0.001
UCS_{wet} (MPa)	0.102	0.555	0.056	0.001	0.099	0.066	0.007	0.016

Table 7
Correlation of UCS with all parameters after the influence of porosity has been extracted

r^2	G_s	Quartz (%)	Feldspar (%)	Rock fragment (%)	GAR (%)	d_{mean} (mm)	FF
UCS_{dry} (MPa)	0.337	0.040	0.013	0.057	0.445	0.404	0.270
UCS_{wet} (Mpa)	0.128	0.361	0.008	0.222	0.115	0.035	0.016

chlorite. A minor content of montmorillite was found in some sandstones.

The mechanical properties of sandstones, including uniaxial compressive strength and Young's modulus, are listed in Table 4. A fairly wide spectrum of mechanical behavior was observed, in which the dry and wet uniaxial compressive strengths vary from 7–86 and 3–45 MPa, respectively. The (dry) strength is thus classified from low strength to medium strength based on ISRM (1981) definition. Significant wetting softening can be observed, either in strength or in stiffness. The strength reduction ratio R ranges from 0.84 to as low as 0.14. That is, some of the Tertiary sandstones may lose almost 90% of strength due to wetting, while others may just lose 20%.

Fig. 5a illustrates a typical failure envelope of dry and wet sandstones tested, and the strength reduction ratio R under various hydrostatic stress conditions is shown in Fig. 5b. It can be seen that wet sandstones tend to have lower shear strength than dry ones, especially at low hydrostatic stress levels, in which the reduction ratio (R) can be as low as 0.3, as shown in Fig. 5b. Upon greater levels of hydrostatic stress, the strength reduction phenomenon seems to be suppressed by the high hydrostatic stress and results in a greater R ($\sim$ 0.8).

In addition to the variation of strength, these sandstones also exhibit distinct features in deformation behavior. As illustrated in Fig. 6, the studied sandstones possess nonlinear volumetric and shear stress-strain behavior. Based on cyclic loading-unloading tests, it was also found that plastic strain could occur prior to the failure state. Last but not least, significant shear dilation occurs when subjected to pure shearing, as shown in Fig. 6c. Meanwhile, two types of deformational behavior have been identified, *types A* and *B*, as schematically illustrated in Fig. 6. Compared to *type A*, *type B* sandstone is characterized by greater degree of deformation (or being "softer") and by having a more significant reduction not only in strength but also in stiffness. This characteristic highlights that *type B* is potentially the rock type prone to tunnel squeezing due to its larger amount of deformation and strength reduction.

4. Influences of petrographic parameters on dry UCS

The results of previous researches have shown that the petrographic parameters, which influence the UCS of sandstone, include mineral composition, grain packing, grain contact, etc. (Bell, 1978; Dobereiner and De Freitas, 1986; Shakoor and Bonelli, 1991; Bell and Culshaw, 1993, 1998; Ulusay et al., 1994; Bell and Lindsay, 1999). These parameters may also have influenced on each other; for instance, greater packing density may result in greater grain contact or porosity. Therefore, prior to evaluating the influence of these parameters, the inter-correlations of the analyzed parameters were investigated and summarized, as shown in Table 5. Table 5 indicates that dry density is closely related to porosity with $r^2 = 0.875$. As a result, dry density was removed from the list of parameters to be analyzed.

Furthermore, it has been of interest to distinguish between the major or the minor parameters influencing the compressible strength and to evaluate the associated influences as well. Accordingly, the correlation of all parameters with UCS of sandstone was then studied, as shown in Table 6, which indicates that porosity n has the strongest correlation with UCS.

After the influence of porosity was removed by the method described in Appendix B, the UCS was found to be strongly affected by GAR among other parameters (Table 7). Accordingly, porosity n and GAR were identified as the major parameters influencing UCS. Therefore, it is assumed the dry UCS (UCS_{dry}) can be approximately expressed in terms of porosity (n) and GAR as:

$$UCS_{dry} = f(n, GAR, \ldots) \cong f_1(n) f_2(GAR) \quad (6)$$

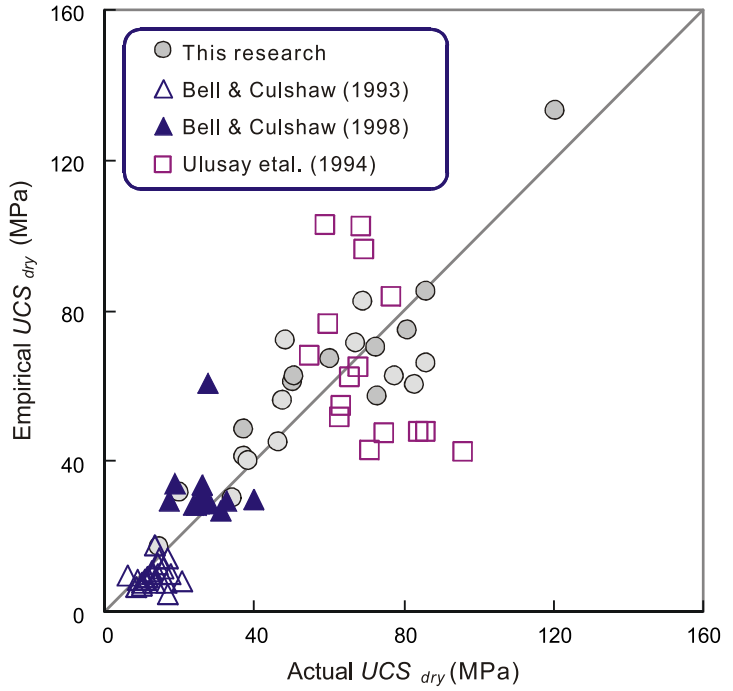

(a) Comparison of actual and empirical *UCS*

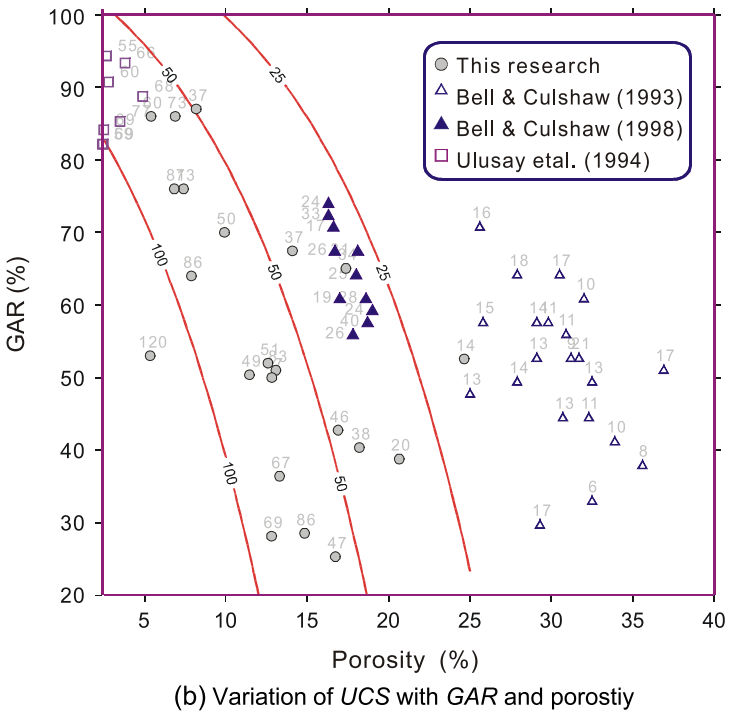

(b) Variation of *UCS* with *GAR* and porostiy

Fig. 7. Comparison of actual UCS with empirical UCS and variation of UCS with GAR and *n*. The actual value of UCS is marked near each symbol in part (b).

The functions $f_1(n)$ and $f_2(\mathrm{GAR})$ can be determined by iterations of regression analysis and are found to be:

$$f_1(n) = 133.7\mathrm{e}^{-0.107n} \quad (7)$$

$$f_2(\mathrm{GAR}) = 3.2 - 0.026\ \mathrm{GAR} \quad (8)$$

Substituting Eqs. (7) and (8) into Eq. (6), the $\mathrm{UCS}_{\mathrm{dry}}$ can be expressed in terms of n and GAR as:

$$\mathrm{UCS}_{\mathrm{dry}} = f_1(n) f_2(\mathrm{GAR}) = (133.7\mathrm{e}^{-0.107n})(3.2 - 0.026\ \mathrm{GAR}) \quad (9)$$

where the units for UCS, n and GAR are MPa, % and %.

If the UCS expressed by Eq. (9) is defined as empirical UCS, it can be compared to the actual UCS, as shown in Fig. 7. In general, the actual UCS and the empirical UCS are closely related (Fig. 7a), with a correlation coefficient (r^2) of 0.765. Although the empirical relation shown by Eq. (9) is obtained for the Tertiary sandstones in Taiwan, it can be used to obtain reasonable estimates of UCS for other sandstones, but with a greater amount of scatter, as shown in Fig. 7a. Since only packing density, but not grain area ratio, were measured by Bell and Culshaw (1993, 1998) and Ulusay et al. (1994), the corresponding grain area ratio for these sandstones was not directly measured but indirectly converted from PD based on Eqs. (4) and (5), which further contributed to the scatter between the actual UCS and the empirical UCS.

Fig. 7b illustrates the variation of UCS with grain area ratio and porosity for all sandstones compared in this work. In Fig. 7b, the contour lines indicate the empirical UCS and numbers near each symbol mark the actual UCS. The sandstones, despite of different compositions, tend to have a greater UCS if they have smaller grain area ratio or porosity.

5. Influences of petrographic parameters on strength reduction

Following a similar process described in Section 4 for obtaining empirical function of $\mathrm{UCS}_{\mathrm{dry}}$, the empirical function for $\mathrm{UCS}_{\mathrm{wet}}$ can be obtained. Furthermore, the strength reduction ratio R owing to wetting softening can be expressed in terms of grain area ratio and porosity as:

$$R = \mathrm{UCS}_{\mathrm{wet}}/\mathrm{UCS}_{\mathrm{dry}} = \frac{36.98\mathrm{e}^{-0.0159n}}{119.9 - \mathrm{GAR}} \quad (10)$$

A comparison of the actual R and the empirical R is shown in Fig. 8a, which indicates a reasonably good agreement between the two R values except for

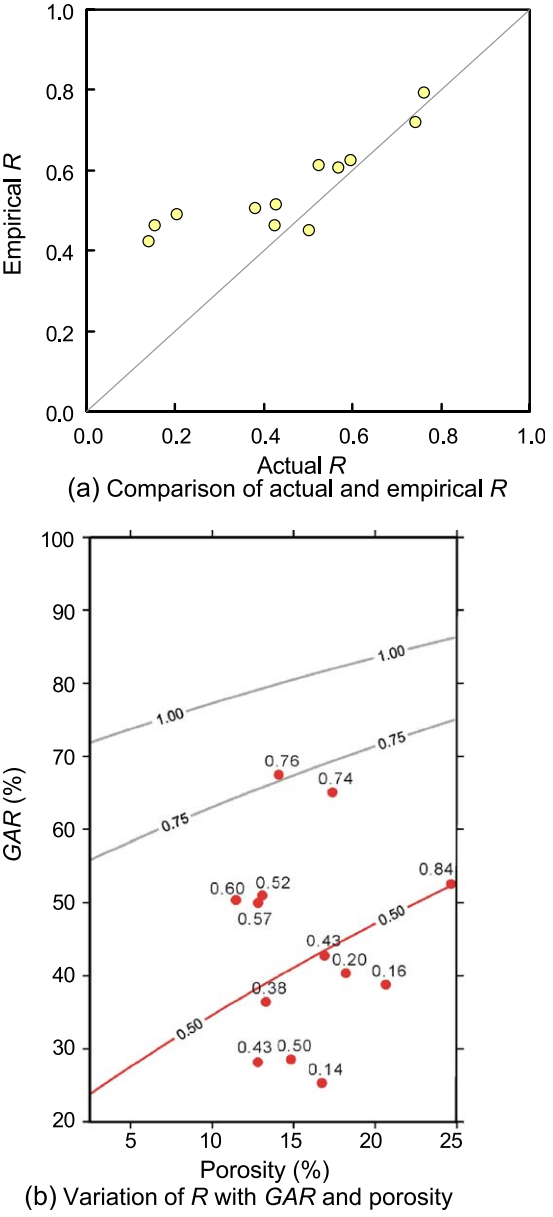

Fig. 8. Comparison of actual R with empirical R and variation of R with GAR and n. The actual R of each sandstone is marked near each symbol in part (b). The magnitudes of empirical R are indicated by the contour lines.

the fact that greater scatter occurs at very low R values (~ 0.2). Similar to UCS_{dry}, R is also affected by n and GAR. Greater n and smaller GAR tend to result in more significant wetting softening, as shown in Fig. 8b.

6. Classification of sandstones based on dry and wet strengths

In order to characterize the studied sandstones, it is necessary to include the wetting softening behavior,

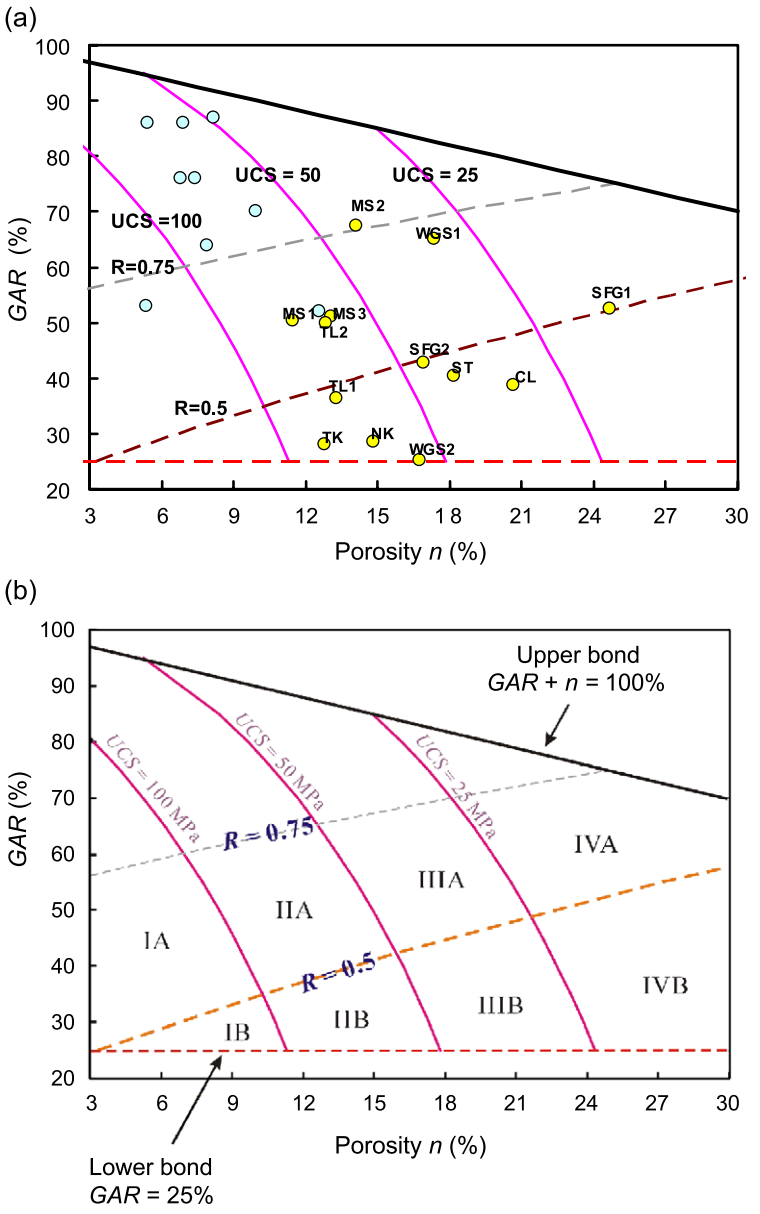

Fig. 9. Proposed geotechnical classification of the studied sandstones in terms of n and GAR. The empirical UCS and R are shown by solid and dashed contour lines. The formation name of each sandstone is marked near each symbol in part (a). Accordingly, the sandstones are classified into two groups: *type A* (R>0.5) and *type B* (R = 0.5) in part (b).

especially when the UCS of both dry and wet sandstones has to be considered in engineering practice. The petrographic analyses have shown that both strength and wetting softening are affected by porosity n and GAR. Therefore, combining all the results shown in Figs. 7 and 8, the influences of n and GAR on UCS and R can be jointly plotted in Fig. 9a. This enables the classification of sandstones according to their macroscopic strength and internal parameters (grain area ratio and porosity). As shown in Fig. 9b, the rocks are classified according to their strengths (UCS_{dry}) as indicated by symbols I, II, III and IV, which correspond to the ISRM (1981) definitions for strong rock, medium rock, moderate strong rock and weak rock, bounded by the strengths of 100, 50 and 25 MPa, respectively.

As far as wetting softening is concerned, in conjunction with the deformational behavior shown in Fig. 6, if $R=0.5$ is selected as the criterion for division of rock types, the geotechnical behavior of Tertiary sandstones can be grouped into two types (indicated as *types A* and *B*), as proposed in Fig. 9b. Based on the proposed definition, the significance of *type B* means one grade down of strength,

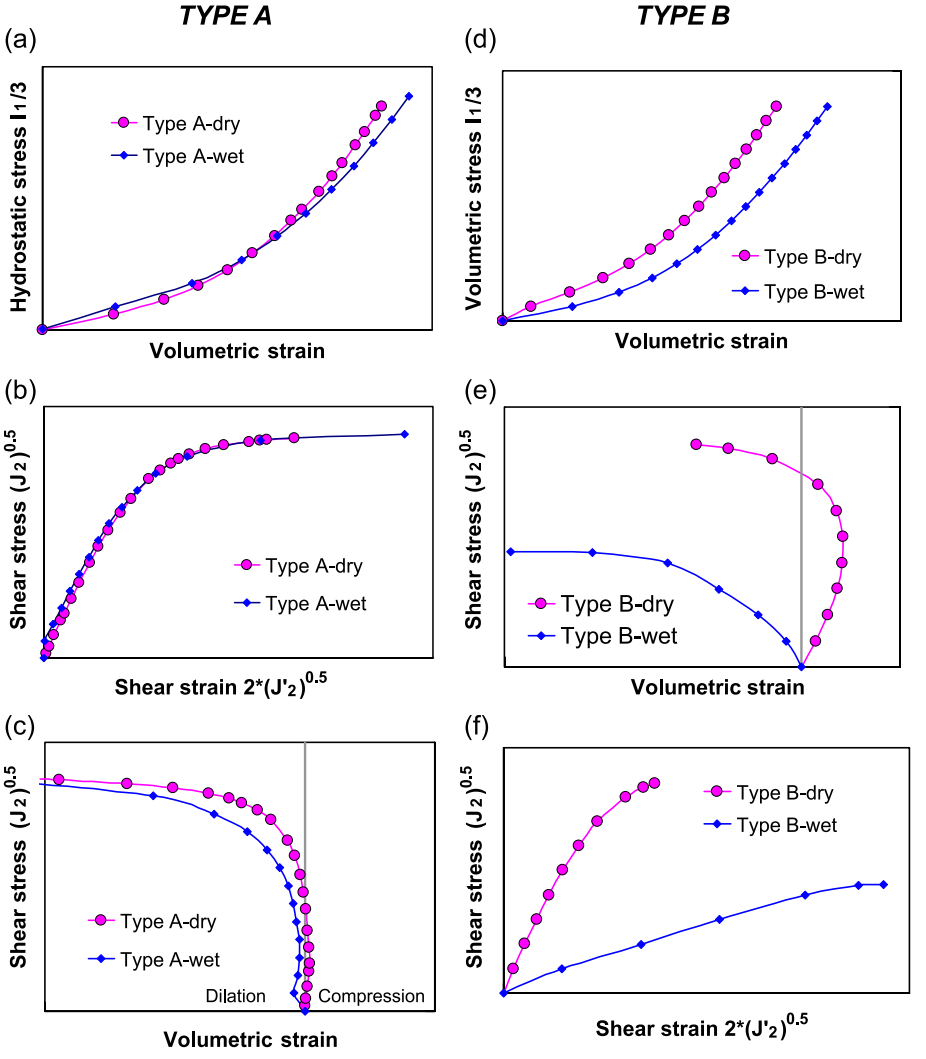

Fig. 10. Influence of wetting on the deformational behavior of type A (MS2) and type B (WGS2) sandstones.

e.g., from *types II* to *III*, when the sandstone gets wetted.

(a) Type A—This group of sandstones has R>0.5, and hence has a relatively less significant wetting softening tendency both in strength and stiffness reduction.
(b) Type B—This group of sandstones ($R \leq 0.5$) is characterized by greater deformation (Fig. 6) and, what is worse, more significant wetting softening. As shown in Fig. 10d, e and f, when type B sandstone is wetted, significant reductions both in strength and stiffness occur. However, the strength and stiffness of type A sandstone is almost not affected by wetting (Fig. 10a–c).

The proposed geotechnical classification chart for sandstones shown by Fig. 9b also indicates that: (a) wetting softening could occur even for sandstones with medium to moderate strengths; (b) same strength, less grain area ratio and greater porosity would induce more significant wetting softening; and (c) less porosity and greater grain area ratio would result in higher strength (and stiffness) of sandstone. Indeed, the phenomenon of less porosity and greater grain area ratio physically represents better compaction of sandstone and high grain content, which is potentially stronger than the matrix especially for the Tertiary sandstones and, as expected, it results in greater UCS and lower degree of wetting softening.

Once the influences of grain content and porosity are identified, the influence of matrix content can readily be found by Eq. (2). On the basis of Fig. 9, the geotechnical properties (UCS and *R*) can be jointly expressed in terms of the constitution of sandstone,

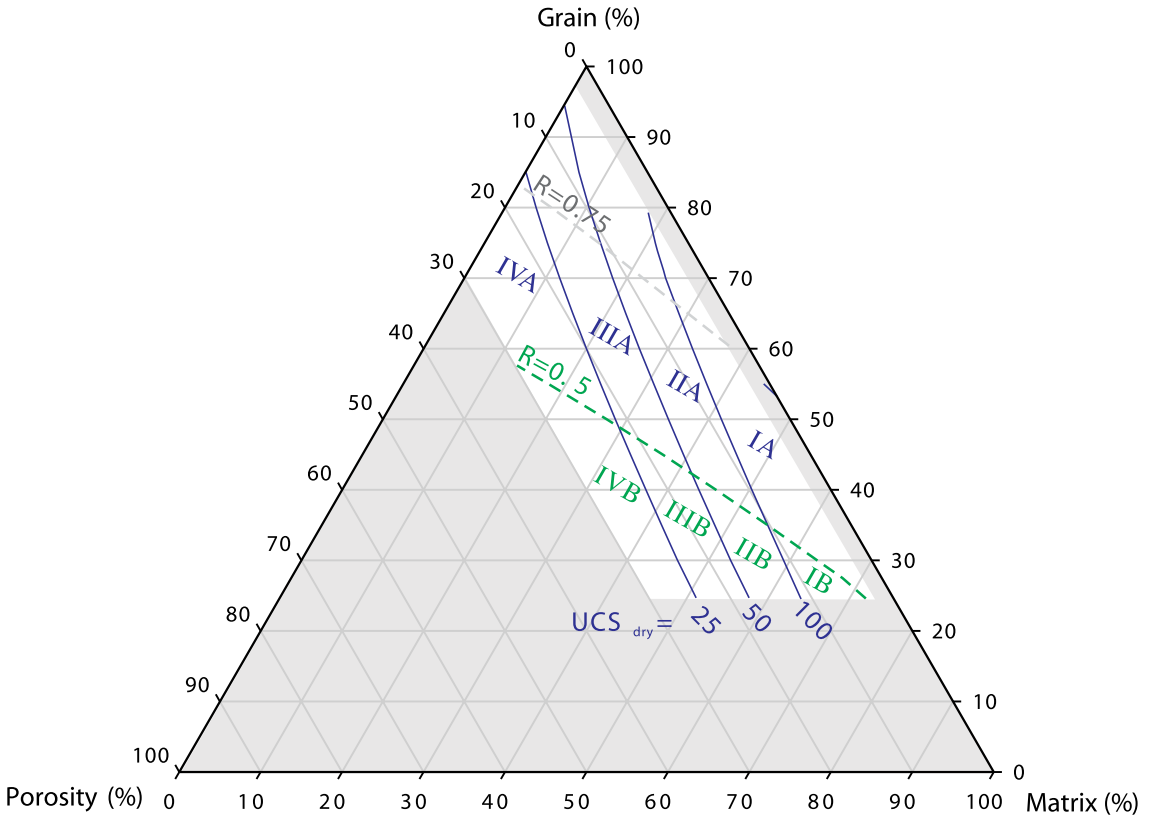

Fig. 11. Relation of the proposed geotechnical classification system with the grain–porosity–matrix content.

namely the grain–porosity–matrix content, as illustrated in Fig. 11. Fig. 11 indicates how the UCS and *R* are affected by the composition of sandstone and reveals that:

(a) Grain area ratio and porosity have about same order of influence on the R;
(b) UCS is mainly affected by porosity, while grain area ratio has less influence, especially at the low to medium levels of grain area ratio; and
(c) At high levels of grain area ratio (e.g., greater that 70%) and constant porosity, increases of grain area ratio (one the other hand, decreases of matrix content) would possibly result in lower strength. A further examination of Fig. 7b shows that such a trend does exist for about two thirds of the cases; however, some exceptions still appear, for instance, for n = 10–15. The exceptional cases indicate that two of the sandstones with greater grain area ratio still have greater UCS. The authors believe that the matrix material and the grain contact should be explored as the possible reason for such exceptions.

7. Conclusion

The adopted experimental technique, including pure shear test and cyclic loadings, allows the geotechnical characteristics of Tertiary sandstone to be revealed. It was found that the Tertiary sandstones could be classified into two groups, *types A* and *B* sandstones. Compared to type A sandstones, type B sandstones tend to have a higher degree of strength reduction due to wetting ($R < 0.5$) as well as more significant deformation, especially shear dilation.

A classification method characterizing the geotechnical properties of sandstones was accordingly proposed. In addition to the commonly used strength (UCS), the strength reduction ratio (*R*) is found to be another important measure used in characterizing the properties of sandstones. The use of these two simple measures, UCS and *R*, and the proposed classification method (Fig. 9) helps the engineering foresee the potential problems to be encountered, for instance, in tunneling.

It has been also found that grain area ratio and porosity are the two key parameters influencing UCS and *R*. It was found that smaller porosity and greater

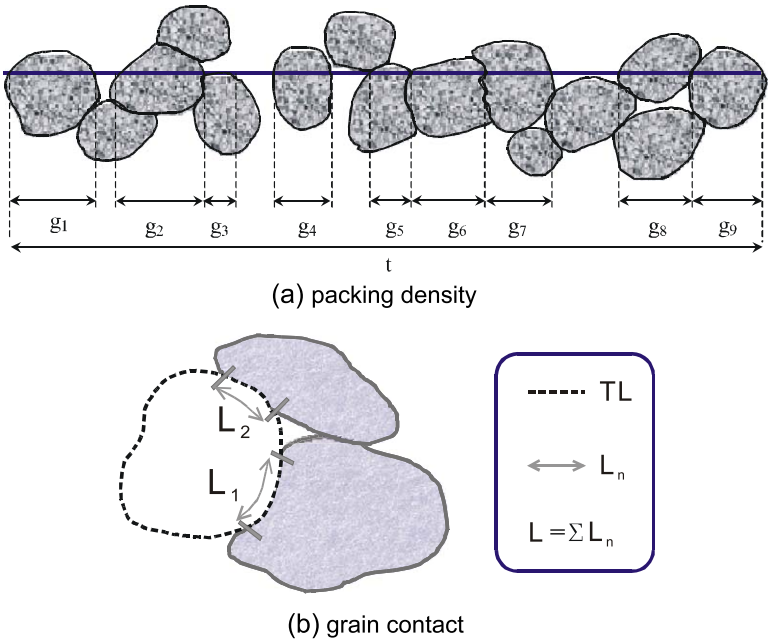

Fig. 12. Schematic illustration on the definitions of packing density and grain contact.

grain area ratio would result in greater UCS. One the other hand, greater porosity and smaller grain area ratio lead to more significant wetting softening. Furthermore, empirical functions of UCS and R, expressed in terms of porosity and grain area ratio, are proposed based on regression analyses. The empirical function of UCS has been compared to other sandstones worldwide from published data. It was found that most of the actual UCS met the empirical UCS, in general.

The proposed classification can also be plotted in terms of the grain–matrix–porosity content, as shown in Fig. 11. This chart shows how the composition of sandstone influences its mechanical properties and geotechnical characteristics. This chart differs from that proposed by Pettijohn et al. (1987) and has more geotechnical significance.

Acknowledgements

The research is supported by the National Science Council of Taiwan, grant nos. NSC-84-2211-E-008-039, NSC-85-2211-E-008-037 and NSC-90-2211-E-002-094.

Appendix A. Definition and determination of petrographic parameters

A.1. Packing density

The packing density (PD), as defined by Kahn (1956), is the ratio of the sum of the grain length encountered along a traverse across a thin section to the total length of the traverse, and PD can be expressed as:

$$\mathrm{PD} = \frac{\sum g_i}{t} \times 100\% \tag{11}$$

where g_i is the grain intercept length of the ith grain in the traverse as defined in Fig. 11a; t is the total length of the traverse.

A.2. Grain area ratio

The GAR is defined as:

$$\mathrm{GAR} = \frac{A_\mathrm{g}}{A_\mathrm{t}} \tag{12}$$

where A_g is the total area of all grains within a reference area and A_t is the total area enclosed by the reference area boundary.

A.3. Grain contact

The GC, as defined by Dobereiner and De Freitas (1986), is the ratio to its own total length of the length of contact a grain has with its neighbors and can be determined as (Fig. 11b):

$$\mathrm{GC} = \frac{\sum L_n}{L} \times 100\% \tag{13}$$

where L_n = length of contact with other grain and L is the total length of boundary of a particular grain.

A.4. Form factor

Form factor (FF) of the grain is defined as:

$$\mathrm{FF} = \frac{4\pi A}{L^2} \tag{14}$$

where A is the area of a grain and L is the length of grain boundary. The values of FF range from close to 0, for very elongated or rough objects, to 1 for a perfect circle.

A.5. Mean grain size (d_{mean})

Mean grain size (d_mean) is defined as the average value of the diameters of all grains in a reference area, which represents the mean grain size.

Appendix B. Methodology for finding empirical functions from several parameters

When a material response (e.g., UCS) is inter-affected by several parameters (e.g., x_1, x_2, …, x_n) in a way that a function F (= UCS) exists, it can be expressed as:

$$F = f(x_1, x_2, \ldots, x_n) \tag{15}$$

The function form of F is unknown; however, it is assumed that F has the following form for the sake of simplicity:

$$F \cong f(x_1)\, f(x_2) \ldots f(x_n) \tag{16}$$

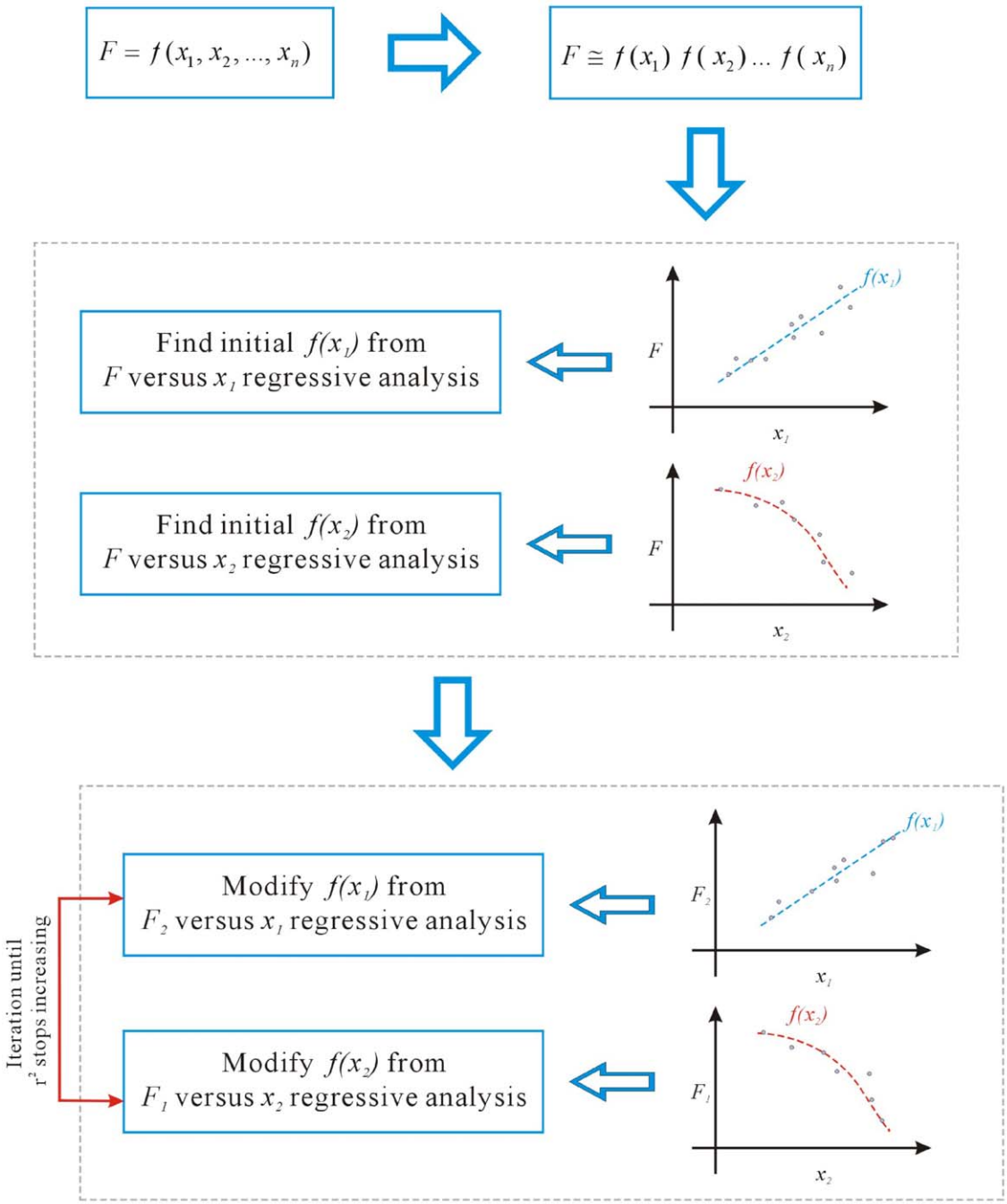

Fig. 13. Flowchart illustrating the process for finding the empirical function of each parameter.

Each function on the right hand side of Eq. (16) represents the magnitude of the influence of each parameter. Empirical functions of $f(x_i)$ can possibly be determined by regression analysis of experimental data. Meanwhile, the degree of influence varies from one parameter to another. It is of interest to find the first most influential function and then the second influential function, and so on. The finding of influential functions will be continued until the remaining parameters have no meaningful influence.

The influence of each parameter has not been known so far; however, it can be found by comparing the influences of each parameter through multivariate regression analyses. Provided that the results of regression analyses indicate that x_1 has the best correlation with F, x_2 is the second and so on to x_n. Then, the function form of $f(x_1)$, $f(x_2)$, …, $f(x_n)$ needs to be determined.

The following iterative process is proposed to obtain the approximate form of the functions. Firstly, the preliminarily $f(x_1)$ and $f(x_2)$ can be found by comparing F with x_1 and x_2, and regression functions, namely $f(x_1)$ and $f(x_2)$, can be determined, as shown in Fig. 12. It should be noted that the determined functions $f(x_1)$ and $f(x_2)$ still influenced by another parameter and such influence can be minimized through the iteration process illustrated by Fig. 12. To extract the influence of x_1, F is then normalized by $f(x_1)$, as below:

$$F_1 = F/f(x_1) = f(x_2)\ldots f(x_n) \cong f(x_2) \tag{17}$$

The function $f(x_2)$ can then be modified by finding the regression function of F_1 with x_2. Similarly, the function $f(x_1)$ can be modified by finding the regression function of F_2 with x_1, which is defined as:

$$F_2 = F/f(x_2) = f(x_1)\ldots f(x_n) \cong f(x_1) \tag{18}$$

The empirical functions of $f(x_1)$ and $f(x_2)$ are continuously modified by the iteration process of Eqs. (17) and (18), until the regressional factor (r^2) stops increasing. Following the same iteration process, other functions $f(x_3)$ to $f(x_n)$ can be accordingly determined (Fig. 13).

References

Aristorenas, G.V., 1992. Time-dependent behavior of tunnels excavated in shale. Doctoral thesis. Dept. of Civil Eng. Massachusetts Institute of Technology, MA, U.S.A.

Bell, F.G., 1978. The physical and mechanical properties of the Fell Sandstones Northumberland England. Engineering Geology 12, 1–29.

Bell, F.G., Culshaw, M.G., 1993. A survey of the geotechnical properties of some relatively weak Triassic sandstones. The Engineering Geology of Weak Rock: Proceedings of the 26th Annual Conference of the Engineering Group of the Geological Society, Leeds, United Kingdom. Balkema, Rotterdam, pp. 139–148.

Bell, F.G., Culshaw, M.G., 1998. Petrographic and engineering properties of sandstones from the Sneinton Formation, Nottinghamshire, England. Quarterly Journal of Engineering Geology 31, 5–19.

Bell, F.G., Lindsay, P., 1999. The petrographic and geomechanical properties of sandstones from the Newspaper Member of the Natal Group near Durban, South Africa. Engineering Geology 53, 57–81.

Bernabe, Y., Fryer, D.T., Shively, R.M., 1994. Experimental observations of the elastic and inelastic behavior of porous sandstones. Geophysical Journal International 117, 403–418.

Besulle, P., Desrues, J., Raynaud, S., 2000. Experimental characterization of the localisation phenomenon inside a Vosges sandstone in a triaxial cell. International Journal of Rock Mechanics and Mining Sciences & Geomechanics Abstracts 37, 1223–1237.

Dobereiner, L., De Freitas, M.H., 1986. Geotechnical properties of weak sandstone. Geotechnique 36 (1), 79–94.

Dyke, C.G., Dobereiner, L., 1991. Evaluating the strength and deformability of sandstones. Quarterly Journal of Engineering Geology 24, 123–134.

Ersoy, A., Waller, M.D., 1995. Textural characterisation of rock. Engineering Geology 39, 123–136.

Handin, J., Hager, R.V., 1957. Experimental deformation of sedimentary rock under a confining pressure. Journal of American Association of the Petroleum Geology 41, 1–50.

Hatzor, Y.H., Plachik, V., 1997. The influence of grain size and porosity on crack initiation stress and critical flaw length in dolomites. International Journal of Rock Mechanics and Mining Sciences 34, 805–816.

Hatzor, Y.H., Plachik, V., 1998. A microstructure-based failure criterion for Aminadav dolomites. International Journal of Rock Mechanics and Mining Sciences 35, 797–805.

Hawkins, A.B., McConnell, B.J., 1992. Sensitivity of sandstone strength and deformability to changes in moisture content. Quarterly Journal of Engineering Geology 25, 115–130.

Ho, C.S., 1986. A synthesis of the geological evolution of Taiwan. Tectonophysics 125, 1–16.

ISRM, 1981. In: Brown, E.T. (Ed.), Rock Characterization Testing and Monitoring—ISRM Suggested Methods. Pergamon, New York, 211 pp.

Jeng, F.S., Huang, T.H., 1998a. Shear dilational behavior of weak sandstone. Proc. of Regional Symposium on Sedimen-

tary Rock Engineering, Public Construction Commission of Taiwan, Taipei, Taiwan, pp. 262–267.

Jeng, F.S., Huang, T.H., 1998b. Time dependent behavior of weak sandstone on Mushan Formation. Proc. of the 13th Southeast Asian Geotechnical Conference, Chinese Institute of Civil and Hydraulic Engineering, Taipei, Taiwan, pp. 75–80.

Jeng, F.S., Ju, G.T., Huang, T.H., 1994. Properties of some weak rock in Taiwan. Proc. of the 1994 Taiwan Rock Engineering Symposium, National Central University, Chungli, Taiwan, pp. 259–267.

Jeng, F.S., Lee, I.T., Huang, T.H., 1996a. Deterioration of weak rock induced by wetting process. Proc. of 1996 Taiwan Rock Engineering Symposium, National Taiwan University, Taipei, Taiwan, pp. 373–382.

Jeng, F.S., Lin, M.L., Huang, T.H., 1996b. Study of the geological barriers of the tunnels in northern Taiwan. Research report MOTC-STAO-RD1501, Ministry of Transportation, Taipei, Taiwan, 127 pp.

Jeng, F.S., Weng, M.C., Huang, T.H., Lin, M.L., 2002. Deformational characteristics of weak sandstone and impact to tunnel deformation. Tunnelling and Underground Space Technology 17, 263–274.

Kahn, J.S., 1956. The analysis and distribution of the properties of packing in sand-size sediments: 1. On the measurement of packing in sandstone. The Journal of Geology 64, 385–395.

Lin, M.L., Hsiuang, H.C., 1998. Microstructure and strength of sandstone in Chaolan formation. Proc. of Regional Symposium on Sedimentary Rock Engineering, Public Construction Commission of Taiwan, Taipei, Taiwan, pp. 113–118.

Pettijohn, F.J., Potter, P.E., Siever, R., 1987. Sand and Sandstone. Springer-Verlag, Berlin. 306 pp.

Plachik, V., 1999. Influence of porosity and elastic modulus on uniaxial compressive strength in soft brittle porous sandstones. Rock Mechanics and Rock Engineering 32, 303–309.

Shakoor, A., Bonelli, R.E., 1991. Relationship between petrographic characteristics, engineering index properties, and mechanical properties of selected sandstone. Bulletin of the Association of Engineering Geologists 28, 55–71.

Tuğrul, A., Zarif, I.H., 1998. The influence of mineralogical textural and chemical characteristics on the durability of selected sandstones in Istanbul, Turkey. Bulletin of Engineering Geology and the Environment 57, 185–190.

Tuğrul, A., Zarif, I.H., 1999. Correlation of mineralogical and textual characteristics with engineering properties of selected granitic rocks from Turkey. Engineering Geology 51, 303–317.

Ulusay, R., Tureli, K., Ider, M.H., 1994. Prediction of engineering properties of selected litharenite sandstone from its petrographic characteristics using correlation and multivariate statistical techniques. Engineering Geology 37, 135–157.